Bioconjugate Chemistry

Article

pubs.acs.org/bc

Spheroid and Tissue Assembly via Click Chemistry in Microfluidic Flow

Paul J. O'Brien, Wei Luo, Dmitry Rogozhnikov, Jean Chen, and Muhammad N. Yousaf*

Department of Chemistry, Centre for Research in Biomolecular Interactions, York University, Toronto, Ontario M3J 1P3, Canada

Supporting Information

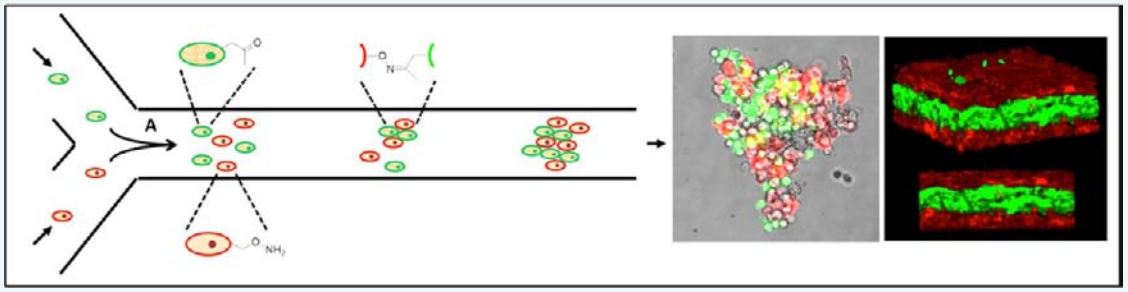

ABSTRACT: Proper cell−cell contact and communication are essential for the correct development and survival of higher order organisms. In order to study complex cell interactions that occur in vivo, model systems that are able to recapitulate 3D cell−cell interactions in vitro are key to advancing new biotechnologies, therapeutics, and tissue engineering applications. Herein, we show a new strategy to rapidly and efficiently generate complex multiple cell line containing spheroids and tissues in microfluidic flow without the use of scaffolds, molecular biology, or metabolic biosynthesis. The method relies on the integration of microfluidics, liposome fusion, bio-orthogonal chemistry, and cell surface engineering to rapidly click coculture cell assemblies in flow. We demonstrate this strategy by assembling various combinations of cell types with an interfacial cell to cell click chemistry in microfluidic flow to generate a range of spheroid types and oriented tissue multilayers.

INTRODUCTION

A major challenge to advance human health is the current inability to generate efficient and cost-effective methods to construct complex three-dimensional multicell types containing spheroids and tissues.[1−3] These in vitro generated spheroids and tissues are crucial for next generation therapeutics to serve as model systems to investigate paracrine and autocrine signaling, tumor growth, and invasion systems that may also be used to generate tissue chips for drug screening and as a method for scaled tissue for organ grafting and replacement therapies.[4−8] Due to the central need for these types of cell based constructs, tremendous progress toward spheroid and tissue formation and paracrine signaling has been made by manipulating cell adhesion properties via molecular biology, non-natural metabolite incorporation through biosynthesis, or the use of polymer scaffolds and decellularized materials.[9−13]

However, a general and inexpensive method to rapidly assemble cells with efficient cell economy would enable new research in systems biology, tissue based biotechnologies, therapeutic tissue chip drug screens, regenerative medicine applications, and in vitro organ construction. This method would require an efficient strategy of delivering chemoselective groups to a cell surface that are able to react with complementary groups on a second cell type to assemble coculture spheroids and eventually complex tissues. In order to develop a general tool to meet these criteria, several design features were required to initiate this research program: (1) a general method which can deliver and label different cell line outer membranes with a range of functional groups without manipulating the genomic content of the cell; (2) a simple bio-orthogonal ligation chemistry that occurs at cell surfaces; (3) ease of synthesis of the lipid like bio-orthogonal groups—these molecules must be straightforward to synthesize and undergo fast and stable bioconjugation at cell surfaces; (4) a fast programmable cell assembly method to generate coculture spheroids with control of cell economy and stoichiometry; (5) the assembly must be scalable, to generate small to large spheroids and tissues with a straightforward stepwise manufacturing assembly line like process; (6) control of orientation of coculture multilayers and degree of thickness of the multilayers; (7) compatible with existing bioreactor, 3D printing, polymer scaffolds, molds, and patterning methods.

Herein, we describe a new platform strategy to rewire cell surfaces with bio-orthogonal groups via a liposome fusion delivery and use microfluidic technology to control the rapid assembly of the coculture microtissues via an interfacial click chemical reaction in flow. The interfacial bio-orthogonal groups delivered to the cell surfaces act as chemoselective molecular velcro to induce a stable but transient click (cell to cell) adhesion process.

Received: July 6, 2015
Revised: August 3, 2015
Published: August 12, 2015

DOI: 10.1021/acs.bioconjchem.5b00376
Bioconjugate Chem. 2015, 26, 1939−1949

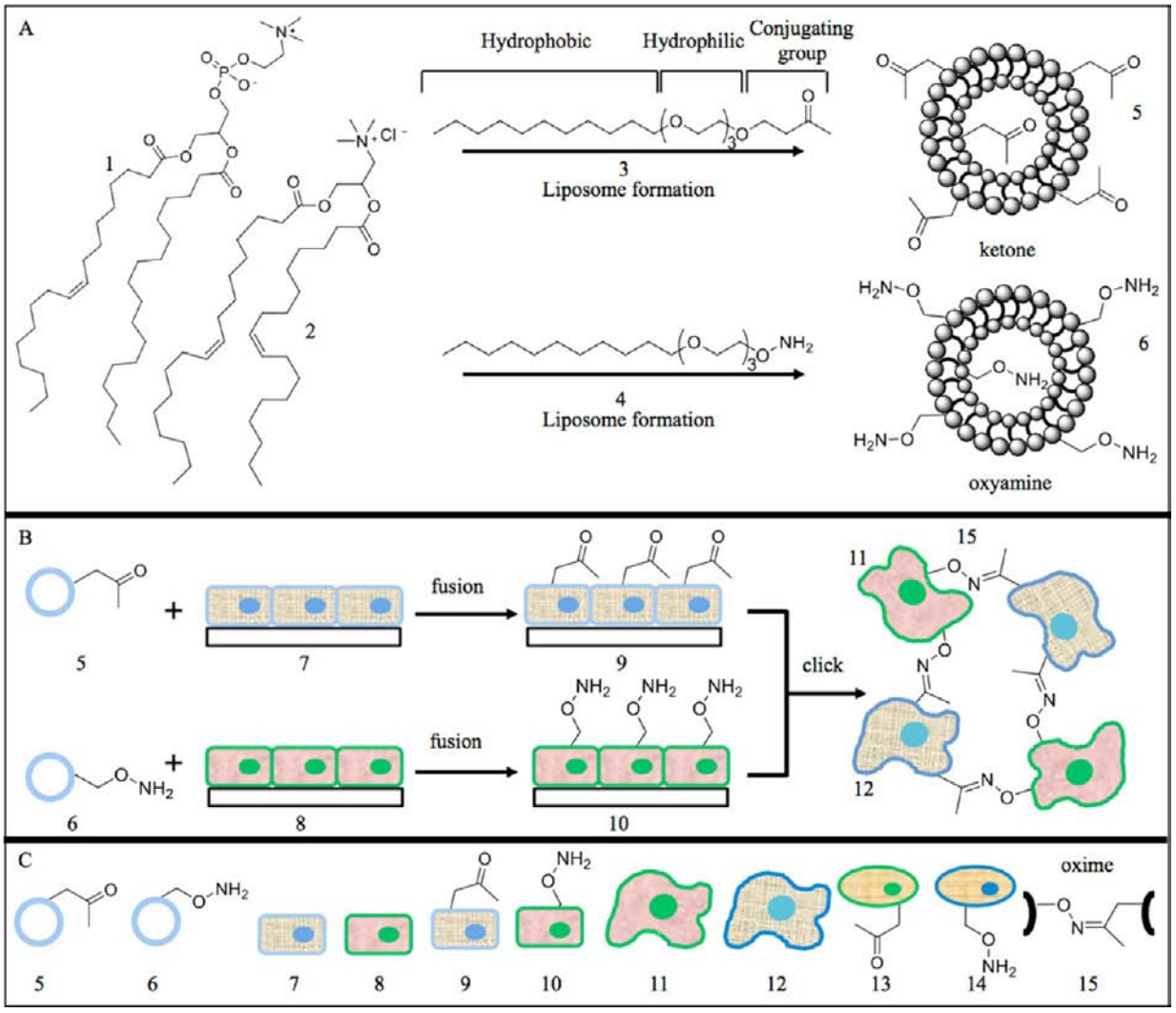

Figure 1. Schematic describing the cell surface tailoring strategy to generate complex coculture tissue assemblies. The combination of bio-orthogonal lipids, liposome formation, and liposome fusion result in the generation of engineered cell surfaces that can subsequently be assembled through an interfacial click reaction. (A) Bio-orthogonal liposomes are formed by mixing POPC (1), DOTAP (2), and either a ketone (3) or oxyamine (4) terminated lipid-like molecules. (B) Cell surfaces (7) and (8) were engineered to present ketones or oxyamines via liposome fusion and delivery. The tailored cells (9) and (10) were then mixed and formed rapid assemblies (11) via the bio-orthogonal oxime (15) click ligation. (C) List of liposomes, cells, and tailored cells used in the study. (5) Ketone tailored liposome, (6) oxyamine tailored liposome, (7) contact inhibited cell line, (8) contact inhibited cell line, (9) ketone engineered cell line, (10) oxyamine engineered cell line, (11) spheroid cell line, (12) spheroid cell line, (13) suspended ketone engineered cell line, (14) suspended oxyamine engineered cell line, and (15) oxime ligation bond between two membrane surfaces.

As a methodology to deliver cargo to cells, liposome formulation and fusion are well established for drug therapeutics and imaging technology.[14,15] Many fundamental studies of lipid membrane fluidity and membrane biology have been advanced by using liposomes as model membranes.[16,17] To rewire cells with the capability to associate with any other cell type we chose to modify cell surfaces with bio-orthogonal lipids as handles for ligation. Bio-orthogonal chemistry is a powerful suite of chemical conjugation reactions that can ligate molecules in a physiological environment rapidly and without side reactions.[18] The reactions have led to pioneering developments with many applications in cell biology and proteomics.[19,20] To control the cell assembly process we used microfluidic technology—a precise bioanalytical method to control spheroid morphology and subsequent tissue orientation. Microfluidic technology has revolutionized biomedical research, and its programmable features have led to diverse innovations in genomics, cell sorting applications, material science, and chemical research.[21−24] However, until now, microfluidic technology has not been used for assembling cells and microtissues in flow due to the relatively weak or nonexistent cell to cell adhesion processes.

RESULTS AND DISCUSSION

To rewire cell surfaces with chemical groups that function as bio-orthogonal molecular velcro, we first focused on the delivery strategy by generating two different liposome populations with complementary ligation groups. Figure 1 describes the cell surface tailoring strategy to generate complex coculture tissue assemblies. We used the reaction between ketone groups and oxyamine groups, which form a stable and bio-orthogonal oxime as the ligation strategy. We have previously shown the utility of this strategy for making coculture spheroids and thick tissue multilayers.[25−28] Each

DOI: 10.1021/acs.bioconjchem.5b00376
Bioconjugate Chem. 2015, 26, 1939−1949

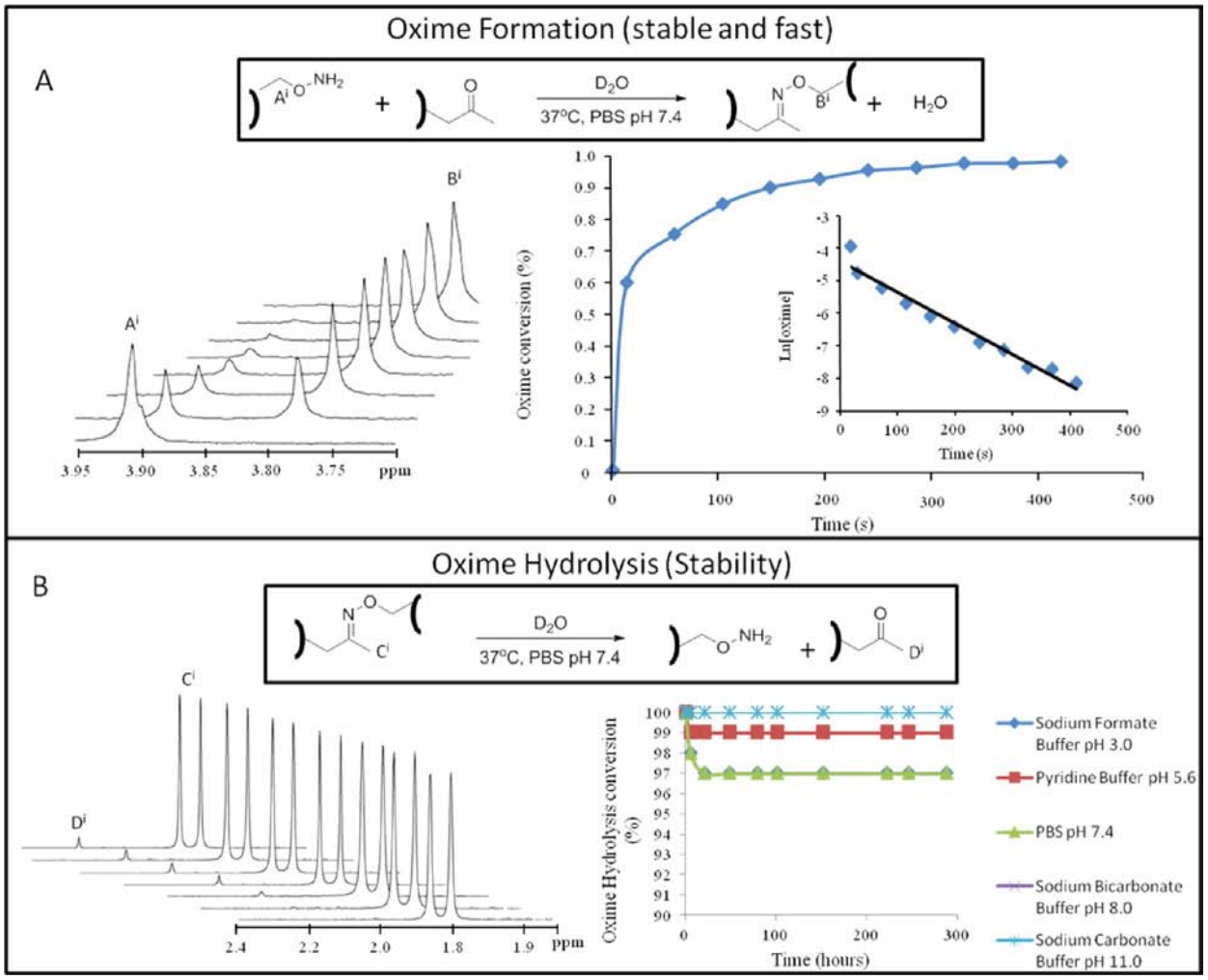

Figure 2. NMR study of the kinetics and stability of bio-orthogonal oxime conjugation reaction under physiological conditions. (A) The reaction of a ketone and oxyamine at physiological conditions (37 °C and pH 7.4) results in the rapid formation of the covalent and stable oxime bond. ^{1}H NMR was used to determine the oxime formation kinetics (k = 0.98 × 10^{-2} M s^{-1}, $t_{1/2}$ = 9 s). (B) The stability of the oxime bond was studied with ^{1}H NMR at physiological conditions (pH 3, 5.6, 7.4, 8.0, 11.0). The oxime bond was stable with no hydrolysis after 3 weeks in pH 3.0 and 5.6. At physiological conditions (pH 7.4) there was only 3% hydrolysis over 3 weeks.

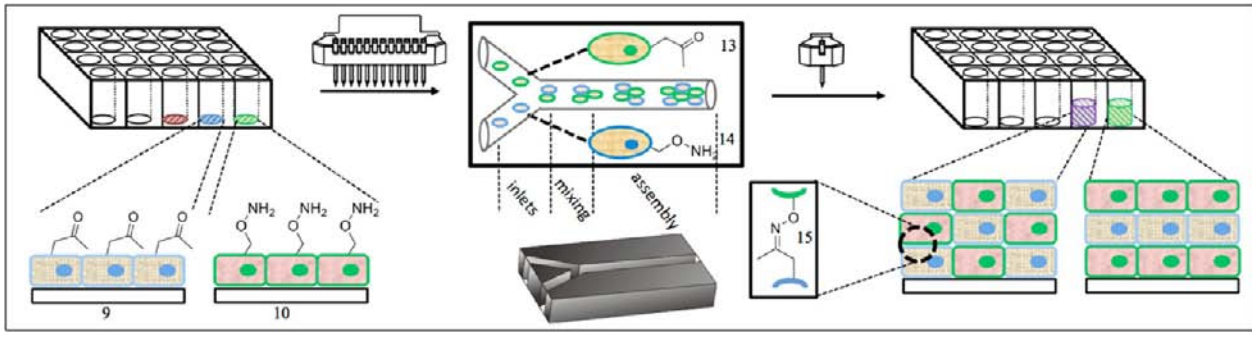

Figure 3. Schematic describing the use of microfluidic technology and tailored cell lines to generate multilayer coculture tissues. (Left) Different cell lines are grown in microwell plates to generate 2D contact inhibited monolayers. Liposomes containing either ketone (5) or oxyamines (6) are added to the microwells. The liposomes rapidly fuse to the cells and deliver the functional groups to rapidly produce engineered cell surfaces presenting ketone (9) or oxyamine (10). (Middle) The engineered cells are then transferred to a simple microfluidic device. As the cells are flown through the channels they come into contact and assemble into coculture spheroids through oxime click chemistry. The sizes of the spheroids are determined by flow rate, cell concentration, and length of assembly chamber. (Right) The spheroids are then transferred to a microwell plate where they adhere and form coculture multilayered 3D tissues. As controls, cells without the bio-orthogonal functional groups produce no spheroids upon mixing in the microfluidic channels and result in no 3D assembly (only standard 2D single cell layer sheets are formed).

liposome pair was generated with background lipids of POPC and DOTAP with the incorporation of either ketone lipid (**3**) or oxyamine lipid (**4**). Once formed, the ketone liposome (**5**) was then added to cells in culture (**7**) containing serum for 1 h

DOI: 10.1021/acs.bioconjchem.5b00376
Bioconjugate Chem. 2015, 26, 1939−1949

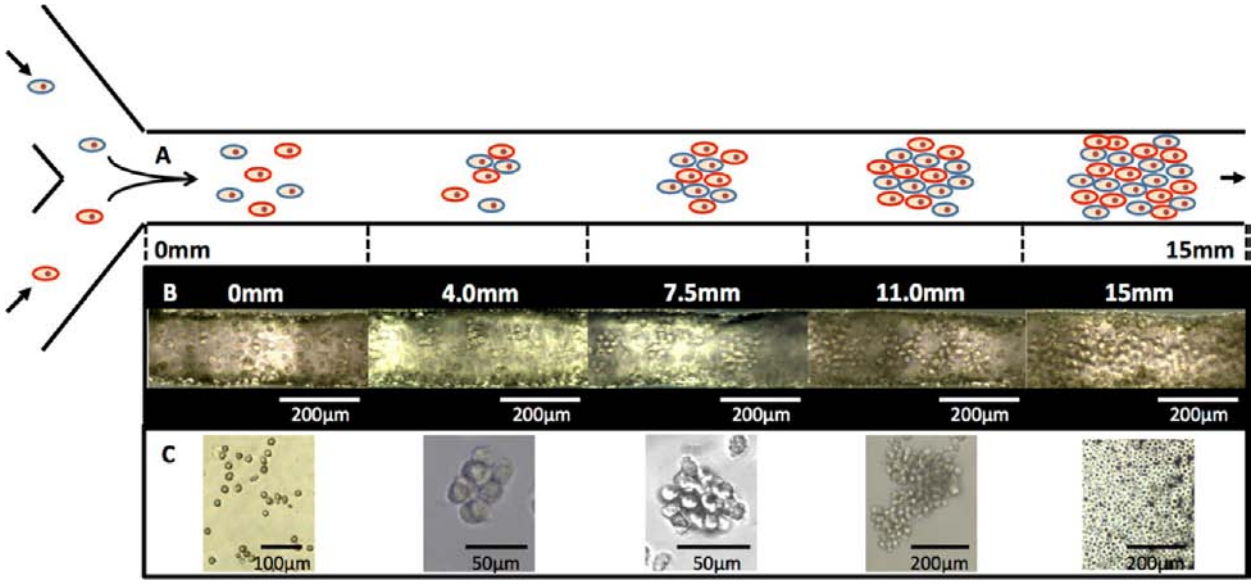

Figure 4. Brightfield images of C3H10T1/2 cells at various stages of assembly in the microfluidic channel device. (A) Cartoon of the PMMA microfluidic device showing the flow of cells in the Y joint followed by mixing and assembly at different lengths of the channel. (B) Brightfield images of representative cell cluster sizes at different flow points along the channel. (C) In situ brightfield images of cells flowing through the microfluidic device at different flow points. Larger spheroid cell assemblies are produced at longer lengths of the channel.

for rapid fusion and delivery of the ketone lipid to the cell surface (**9**). Similarly, oxyamine liposome (**6**) was added to a second cell type to generate oxyamine presenting cells (**10**). Upon the mixing of ketone (**9**) and oxyamine (**10**) presenting cells rapid coculture cell assemblies formed due to the fast and polyvalent oxime click chemistry ligation between cells. As controls, no cell assemblies were generated when either the ketone or oxyamine groups were not present on the cell surface (Supporting Movies S1, S2, S3, S4). FACS analysis was also used to determine the amount of bio-orthogonal lipid present on the cell surfaces.[25] Previous studies have shown that cell viability is not affected by the liposome fusion method or the incorporation of bio-orthogonal lipids into membranes.[26−28] Over time, the cells proliferate and dilute the bio-orthogonal lipid similar to a transient transfection process. The initial oxime ligation nucleates the adhesion between cells and over time the cells proliferate and dilute the bio-orthogonal lipids, but during this process, they excrete extracellular matrix, which in turn holds the tissue together.

In order to rapidly generate coculture assemblies based on bio-orthogonal ligation chemistry in microfluidic flow, we required the intercell surface reaction to be fast and stable. Several bio-orthogonal strategies were available, including Diels-Alder and Huisgen 3 + 2 copper catalyzed cycloadditions, but we chose oxime ligation involving the reaction between oxyamine and ketone groups due to the ease of incorporating those groups into simple lipid like molecules.[25,26] Figure 2 describes the kinetics of formation and stability of the oxime reaction at physiological conditions (pH 7.4, 37 °C). In solution, a model reaction forms the oxime with a half-life of approximately 9 s and is stable for many weeks with minimal hydrolysis. However, we surmised that on the surface of a cell, oxime formation would be several orders of magnitude faster due to the polyvalent nature of surface chemistry and the membrane fluid mosaic ability for the ketone and oxyamine lipids to rapidly diffuse and therefore dramatically change their local concentration density on the cell surface.[29]

Figure 3 shows a schematic describing the overall strategy to generate coculture assemblies in microfluidic flow. First, multiple different cell lines are cultured in microwell plates as single monolayers. To these cell cultures liposomes with either ketone or oxyamine groups were added, which rapidly fuse and tailor the cell surfaces. These cells are then detached and transferred to a standard Y joint microfluidic device. The microfluidic device was made through straightforward PMMA microfabrication. Each arm of the microfluidic channel streamed a different cell line tailored with either the ketone or oxyamine group. As the cells flow through the channels they arrive at the mixing chamber where they come into contact (collide) instantly, forming adhesions due to the intercell bio-orthogonal oxime ligation. As the spheroid assemblies flow through the channel they associate with more cell clusters to generate larger spheroids. As the microtissues flow through the channel they are deposited onto microwells and stack to form 3D multilayer tissues. This microfluidic and cell surface engineering strategy allows for the rapid assembly of complex coculture tissues for studies of spheroid autocrine and paracrine signaling, tumor models, and the formation of 3D multilayer tissues for a range of applications. Controls clearly show that no cell assemblies form when cell surfaces do not present the oxime pair. Furthermore, only monolayer or single cells in solution are generated when either the ketone or oxyamine is not present on the cell surfaces.

Figure 4 shows various images of the size of spheroids along the channel and Figure 5 describes the relationship between spheroid size generated versus flow rate and the position within the channel. As the flow rate decreases and the position along the channel increases the size of the spheroid clusters become larger. It is remarkable that the oxime ligation chemistry between cells is able to hold cells together while flowing through the microfluidic channel. These spheroids and multilayers are stable, do not fall apart, and do not need the support of being entrapped in Matrigel or some other polymer based scaffold (see SI figures S1−S4 for tissue viability and spheroid formation and viability studies).

DOI: 10.1021/acs.bioconjchem.5b00376
Bioconjugate Chem. 2015, 26, 1939−1949

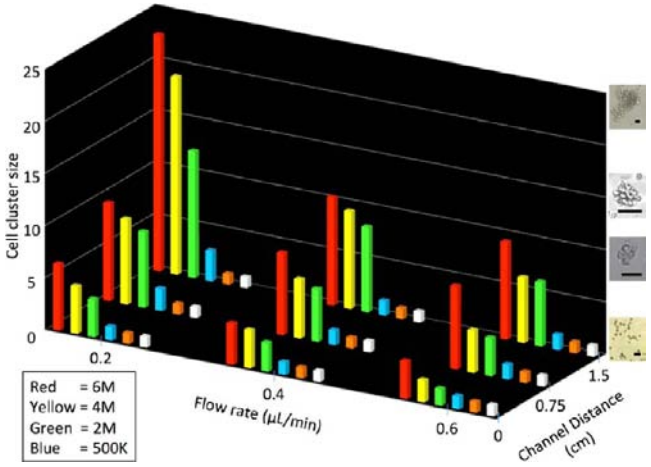

Figure 5. 3D plot presenting the relationship between flow rate, channel distance, cell density, and resulting cell cluster size (spheroid) assembled within a microfluidic channel. As the cell density increases and flow rate decreases spheroids assemble at a faster rate. The absence of one (orange) or both (white) surface chemistries results in no spheroid formation. Statistical analysis showed cluster size was within 5% for each condition.

To generate a range of coculture spheroids by microfluidic assisted assembly, we used several fluorescent cell lines tailored with the bio-orthogonal lipids. Figure 6 shows a cartoon description of the polyvalent nature of the intercell coculture oxime spheroid assembly. Green fluorescent protein (GFP) and red fluorescent protein (RFP) cells were used to demonstrate the assembly of coculture cells in flow. By adjusting the ratio (stoichiometry) of initial cell density, the two cell types formed many different coculture assembly combinations. For example, an 8:1 ratio of GFP to RFP cells flowing through the channels resulted in spheroids containing a single RFP surrounded by GFP cells. Figure 6E shows three cell types forming spheroids by combining equal numbers of RFP−ketone, GFP−ketone, and blue live-dye−oxyamine cells. Figure 6F,G shows GFP and RFP cells forming spheroids based on two sets of the cells with complementary ketone and oxyamine cell surface chemistry. Figure 6H shows fluorescent and brightfield combined images of 1:1 RFP and GFP cell spheroids. By adjusting the flow rate, cell density, cell type, and stoichiometry (ratio) of the cells different combinations of spheroids may rapidly be constructed. These assemblies are fast forming, stable, and do not require the use of a polymer scaffold or hydrogels to ensure spheroid integrity. Furthermore, without the ketone or oxyamine groups on the cell surfaces, no spheroids were formed and only single cells were observed.

To demonstrate the flexibility of the methodology, several coculture assemblies were generated via microfluidic flow and evaluated. Figure 7A,B shows a control monolayer of GFP expressing cells contact-inhibited in culture. Without the bio-orthogonal click chemistry on the cell surface, most cells adhere and proliferate until they become contact-inhibited and form a single monolayer in the $x-y$ plane zone in culture. These cells do not grow on top of each other (in the Z vertical direction) in normal standard cell culture in vitro conditions. However, upon delivering bio-orthogonal lipids via liposome fusion the cells will now form coculture multilayers in the Z (vertical) direction to form multilayers (3D tissues). Figure 7C,D shows confocal images of RFP and GFP cells assembled sequentially in microfluidic flow and then deposited onto cell culture dishes to generate oriented coculture layers. Figure 7E−H shows that complex zones of varying thickness of multiple cell lines (GFP and RFP) can be generated by simple alteration of the amount of cells and sequence of cell deposition. Figure 7I,J shows confocal images of thick multilayers. By depositing many cells onto each other via bio-orthogonal chemistry, thick layers can be formed. The thick tissues are stable and the cells proliferate. As described previously, the ketone and oxyamine lipids dilute over time on the cells via a transient transfection model, but extracellular matrix is generated by the cells. Therefore, the oxime chemistry is slowly diluted and the extracellular matrix holds the tissue layers together. Figure 7K,L shows a thick multilayer of HMSC and fibroblast cells that can be induced to differentiate to different lineages based on the orientation of the cells within the multilayer (for stem cell studies, see Figure 8). Figure 7M,N shows the formation of three cell types in a mixed multilayer via bio-orthogonal chemistry. RFP and GFP engineered with ketone were mixed with blue (CMAC) stained oxyamine cells and assembled as spheroids in microfluidics and then deposited on tissue culture plates to generate 3D mixed multilayers of three cell lines. Figure 7O,P shows the combination of the cell assembly click strategy combined with collagen scaffolds. Upon cell seeding, the collagen scaffold is filled with cells almost instantly due to the ability of the bio-orthogonal cells to simultaneously adhere to each other and to the collagen scaffold. This strategy allows for a very high cell seeding density, which causes rapid filling of polymer scaffolds or decellularized materials.

Figure 8 shows how a polymer-scaffold free stem cell multilayers generated via the microfluidic assembly process could be used to study differentiation of stem cells in 3D coculture. Ketone and oxyamine presenting hMSC cells were mixed with Swiss 3T3 fibroblasts respectively and induced to differentiate to adipocytes, fibroblasts, or osteoblasts via the corresponding induction conditions. The multilayer cocultures were assembled and assayed after 1 day and 2 weeks to determine differentiation lineage. As shown in Figure 8A−F, the 3D cocultures were stable over long periods and the corresponding gene markers were assayed for differentiation lineage specification. This demonstration shows the utility of the coculture system to study how the influence of a second cell type may alter the rate and final differentiation lineage of the stem cells.

CONCLUSION

In summary, we have developed a straightforward and flexible strategy to rewire cells with bio-orthogonal chemical groups that rapidly generate coculture cell assemblies in flow via a fast intercell click reaction. Liposome fusion delivery of the bio-orthogonal lipid like groups to the cell surface is efficient, fast, and inexpensive. The cell surface oxime ligation strategy is kinetically well behaved, stable, and allows for rapid complex coculture and multilayer tissue construction. It is also straightforward to incorporate existing cargo strategies within the liposomes for simultaneous delivery of payloads and bio-orthogonal lipid molecules to surfaces for multiplex applications ranging from imaging to theranostics.[30] Due to the flexibility of the methodology, many other click chemistry reactions may be used and multiple different click chemistries can be incorporated on cell surfaces simultaneously.[31] These methods can be used to tailor surfaces with a range of molecules, probes, biomolecules, and nanoparticles. Because there is no molecular biology or metabolic biosynthetic manipulation of the cells, a

DOI: 10.1021/acs.bioconjchem.5b00376
Bioconjugate Chem. 2015, 26, 1939−1949

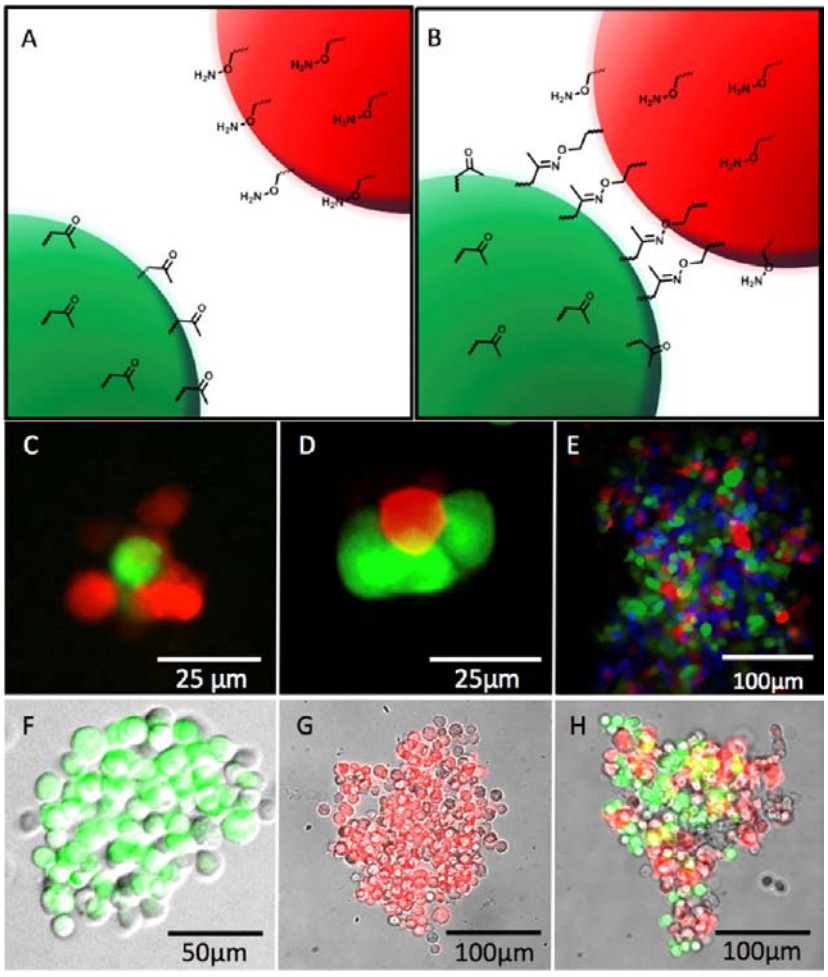

Figure 6. Schematic cartoon and fluorescent images of resultant coculture spheroid assembly via click chemistry ligation. (A) Two cell lines engineered with complementary interfacial bio-orthogonal groups where upon contact undergo click oxime ligation (B) resulting in coculture assembly. (C,D) Changing the engineered cell density ratio injected into the microfluidic device results in spheroids with different morphologies. A 1:8 ratio (GFP:RFP) of cells results in a single GFP NIH 3T3 cell surrounded by RFP Neonatal Dermal Fibroblast cells (C). Reversing the ratio to 8:1 (GFP:RFP) results in a single RFP Neonatal Fibroblast cell surrounded by GFP NIH 3T3 cells (D). (E) Fluorescent image of large 3 cell type spheroid, generated by mixing 1:1:1 ratio of GFP:RFP:Blue C3H10T1\2 stained with CMAC (7-amino-4-chloromethylcoumarin) in flow. These third cell tissues were easily generated by engineering GFP and RFP cells with ketones while CMAC stained cells present oxyamine groups. (F) Large spheroid of GFP cells obtained by combining two different populations of GFP cells that present ketone and oxyamine groups. (G) Large spheroid of RFP cells obtained by combining two different populations of RFP cells that present ketone and oxyamine groups. (H) Large spheroid of RFP and GFP cells obtained by flowing a 1:1 ratio of engineered RFP and GFP cells in the microfluidic device. By adjusting the flow rate, cell density, and ratio of cell density inputs, a range of stoichiometric coculture spheroid assemblies and spheroid sizes could be generated.

large scope of new cell surface capabilities may be possible through bio-orthogonal conjugation. Furthermore, new autocrine, paracrine, tissue, or spheroid studies and regenerative medicine applications are now possible due to the ease of delivery and manipulating cell surfaces. By adopting more complex microfluidic technology, it may be possible to deliver functionalized liposomes and therefore engineer cell surfaces in flow for immunotherapy and nucleic acid based transfection applications.[32] The methodology is complementary to polymer scaffold based tissues by allowing for the rapid filling of the scaffold with cells via the ability of the rewired cells to adhere to each other and to the polymer. The ability to generate multicell type spheroids and thick multilayers may have utility in generating various skin (oriented cell multilayers) and tissue chips (liver) for drug screening or tissue replacement (heart, lung, etc.) therapies.[33−35] Furthermore, many coculture cell lines may be used to generate complex spheroids for cancer tumor model studies. The ability to associate any cell type with stem cells may also lead to new stem cell signaling and differentiation studies. The methodology is also compatible with existing 3D printing technology since the tailored cells may act as the "ink" in the printing process.[36] Finally, due to the efficient cell assembly, a range of different sized tissues with multiple cell lines may be generated in short time periods for imaging and regenerative medicine applications.[10,37]

■ EXPERIMENTAL SECTION

O-Dodecyloxyamine-tetra(ethylene)glycol was synthesized as previously described.[25,26] 1-Palmitoyl-2-oleoyl-*sn*-glycero-3-phosphocholine (POPC) and 1,2-dioleoyl-3-trimethylammonium-propane (DOTAP) were purchased from Avanti Polar Lipids (Alabaster, AL). All other chemicals were obtained from Sigma-Aldrich or Fisher Scientific. 3T3 Swiss albino mouse fibroblasts, C3*H*/10T1/2 mouse embryonic fibroblast cells, RFP Expressing Human Neonatal Dermal Fibroblasts, and GFP expressing NIH3T3 cells were obtained from ATCC. Human

DOI: 10.1021/acs.bioconjchem.5b00376
Bioconjugate Chem. 2015, 26, 1939−1949

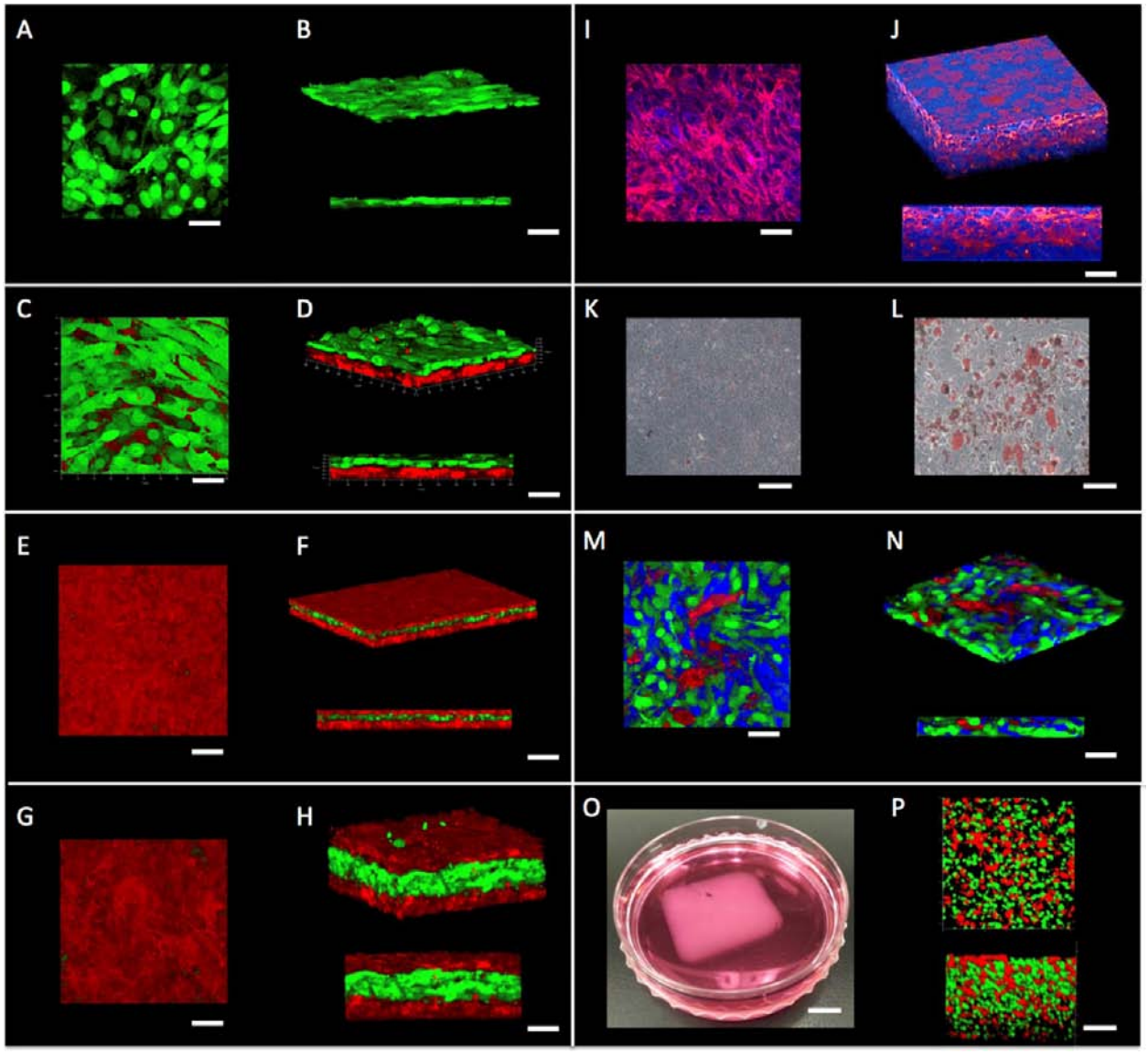

Figure 7. Range of confocal and bright-field images of various combinations of GFP NIH 3T3 fibroblasts, RFP neonatal fibroblasts, CMAC live stained C3H10T1/2 pluripotent embryonic fibroblast stem cells. hMSC cells and NIH Swiss 3T3 cells. (A) Top view of a standard contact inhibited single monolayer of GFP NIH 3T3 cells in culture. (B) Angled and side view of monolayer showing a thickness of approximately 6 μm. (C) Top view image of RFP-GFP bilayer generated by first assembly in microfluidic flow of RFP spheroids followed by deposition onto glass slides to generate RFP multilayer. To this RFP multilayer was added GFP spheroids generated in microfluidic flow. The sequential spheroid and multilayer generation resulted in a bilayer of multilayers of GFP and RFP cells (30 μm thick). (E,F,G,H) Image of serial RFP and GFP spheroid assembly in flow followed by sequential deposition resulted in control of coculture orientation multilayers and thickness (E,F, 30 μm thick) (G,H, 120 μm thick). (I,J) Image of TRITC and DAPI stained thick multilayers of Swiss 3T3 fibroblasts (140 um thick). (K,L) Brightfield image of multilayers of HMSC cells mixed with Swiss 3T3 fibroblasts. (L) After culturing for 10 days the HMSC cells differentiated to adipocytes in the coculture. (M,N) Image of mixed multilayers of 1:1:1 RFP:GFP:Blue C3H10T1/2 cells generated by assembly in flow followed by deposition onto glass slides: The RFP and GFP cells represented ketones and the blue cells represented oxyamines. (O) Photograph of a 2 cm × 2 cm × 0.5 cm thick collagen tissue containing RFP-ketone and GFP-oxyamine cells. Spheroids of RFP and GFP cells were generated in flow and then mixed with collagen. (P) Confocal top and side views of coculture cells in collagen. High cell density within collagen was achieved by the adhesion of large spheroids. The cells adhere to the collagen and to each other, therefore generating high cell density thick tissue instantly.

mesenchymal stem cell (hMSC), hMSC basic, growth, and differentiation media were obtained from Lonza.

Cell Culture. C3*H*/10T1/2 were cultured in Petri dishes at 37 °C and 5% CO_2 with DMEM media containing 10% fetal bovine serum (FBS) and 1% penicillin/streptomycin (P/S). RFP Expressing Human Neonatal Dermal Fibroblasts (RFP) were maintained in DMEM containing 10% FBS and 1% P/S. The cell cultures used for experiments were between 3 and 8 passages. GFP expressing NIH3T3 (GFP) cells were cultured in DMEM (high glucose), with 10% FBS, 0.1 mM MEM Non-Essential Amino Acids, 2 mM L-glutamine, 1% P/S, and 10 μg/mL Blasticidin. 3T3 Swiss albino mouse fibroblasts were cultured in Dulbecco's Modified Eagle Medium (Gibco) containing 10% FBS and 1% penicillin/streptomycin at 37 °C in 5% CO_2. hMSCs were cultured in growth media at 37 °C in 5% CO_2. Adipogenic differentiation was induced by adipogenic induction medium and kept by induction/maintenance cycles as described in the Lonza protocol. Osteogenic differentiation

DOI: 10.1021/acs.bioconjchem.5b00376
Bioconjugate Chem. 2015, 26, 1939−1949

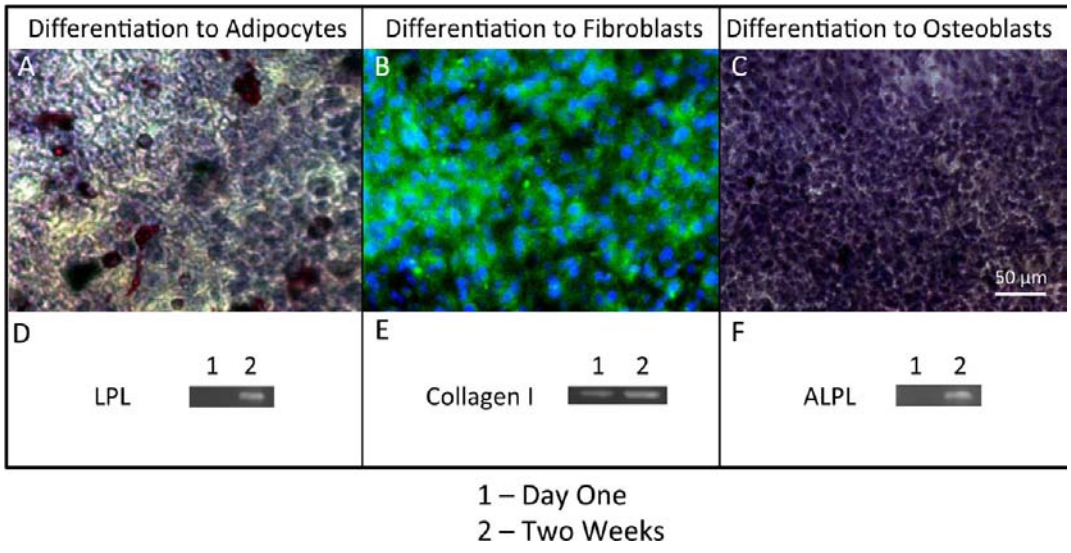

Figure 8. Construction of a 3D tissue coculture system via intercell click ligation and application to stem cell differentiation. (A–C) Coculture system of hMSCs/fibroblasts were assembled and then made to differentiate to adipocytes (A), fibroblasts (B), and osteocytes (C) via corresponding induction conditions. Adipocytes, fibroblasts, and osteoblasts were stained red, green, and blue, respectively. Images were taken by 20× phase contrast microscopy. Corresponding gene makers (LPL for adipocytes, Collagen I for fibroblasts, ALPL for osteoblasts) were studied over 2 weeks. (1, day one; 2, 2 weeks) and are represented by the gels as shown in D, E, and F, respectively.

was induced by osteogenic induction medium provided by Lonza.

Microfluidic Device Fabrication and Design. The microchannel was designed with a simple Y-shape, where cell suspensions are brought together in the Y-joint mixing zone. In order to make a simple, cheap, and robust device, PMMA blocks were used as the device substrate. The experimental device was fabricated using laser ablation to etch PMMA blocks (1/8 in thickness, 1.25 in length, and 1.42 in width). The PMMA channels were laser etched using Versalaser 2.30 with a CO_2 laser at 14.25 W power to produce parabolic channels with a measured base width of 170 μm, a peak height of 200 μm, and a channel length of 1.5 cm. The fluid inlet connections were fabricated using 406 μm (0.016 in) OD stainless steel capillary tubes with an 203 μm (0.008 in) ID and a length of 2.0 cm, which were embedded into the PMMA blocks using thermal heating to be in line with the channel flow axes, while the fluid outlet capillary was cut to 2.0 cm and embedded by thermal heating and pressure similarly to the fluid inlets and allowed to cool. The top block of PMMA is used to cap the channel through thermal bonding with the etched bottom block in a convection oven for 2 h at 275 °C and allowed to cool completely to room temperature over 2 h under pressure. Once cooled, the fluid connections are finished by slipping PEEK tubing (ID 203 μm/0.008 in) over the metal capillary and sealed using epoxy resin (3M). Finally, high pressure HPLC 1 mL Luer lock glass syringes (Hamilton) are connected to the PEEK tubing using finger tight female Luer fittings (UpChurch Scientific).

Liposome Formation and Formulation. To prepare liposomes bearing ketone or oxyamine functionalities, 60 μL 2-dodecanone-tetra(ethylene)glycol (10 mM in $CHCl_3$) or *O*-dodecyloxyamine-tetra(ethylene)glycol (10 mM in $CHCl_3$) was mixed with 430 μL POPC (10 mg/mL in $CHCl_3$) and 10 μL of DOTAP (10 mg/mL in $CHCl_3$), and then thoroughly dried via N_2. After the $CHCl_3$ was evaporated, the lipid mixture was suspended in 3 mL of PBS, followed by tip sonication for 15 min until the suspension became clear.

Cell Surface Modification Using Liposome Fusion. Once cells reach 90% confluency, 5% (v/v) liposomes (ketone or oxyamine bearing liposomes) were added to the cell culture media, and incubated with cells at 37 °C and 5% CO_2 for 1 h to create ketone- or oxyamine-tailored cells.

General Method for Spheriod Generation in Microfluidic Device. GFP NIH 3T3 and RFP HNDF cells were grown to approximately 90% confluency and then treated with oxyamine and ketone bearing liposomes, respectively, using the standard protocol. Once the cells were surface engineered, they were washed 3 times with PBS and then detached using 0.25% trypsin/EDTA at 37 °C and 5% CO_2. Once the cells were detached and neutralized by DMEM media (10% FBS), cell suspensions were transferred to separate 15 mL centrifuge tubes and centrifuged down at 800 rpm for 5 min. The supernatant was discarded and the remaining pellet was resuspended in DMEM media to reach a final concentration of 4×10^6/mL. Once the ketone and oxyamine-tailored cell suspensions were ready, 250 μL of each cell suspension was immediately loaded into separate sterilized 1 mL gastight Luer lock Hamilton gas chromatography syringes. The connection tubing and microfluidic device were sterilized by passing 1 mL 70% ethanol solution, followed by 1 mL of PBS buffer. Once sterilized, the loaded syringes were finger tightened onto male Luer connections and placed onto a Harvard 11 PLUS syringe pump. The flow rate was set to 8 μL/min for 5 min to purge air bubbles from the system, then reduced to 0.4 μL/min for 5 min, where the fluid was discarded and subsequent eluent was collected onto 1 cm^2 glass slides. The 1 cm^2 glass slides were prepared in advance and sterilized by sonication in 70% ethanol solution for 30 min. The microfluidic experiments typically lasted around 45 min. After experiments were done, the collecting slides were transferred to tissue culture plates and incubated at 37 °C and 5% CO_2 for 25 min. The cells on the slides were then fixed by 3.8% formaldehyde solution for 15 min, followed with gentle washing with PBS. The cell samples were observed and imaged using a Nikon Eclipse TE2000-U Fluorescence Microscope.

DOI: 10.1021/acs.bioconjchem.5b00376
Bioconjugate Chem. 2015, 26, 1939–1949

Engineered Spheriod Growth Kinetics Using Microfluidics. C3*H*/10T1/2 cells were cultured to approximately 90% confluency and engineered using standard conditions. Once the cells were detached, the suspension would be diluted using serum containing growth medium to obtain different cell densities; 250 μL of each cell suspension was immediately loaded into separate sterilized 1 mL gastight Luer lock Hamilton gas chromatography syringes. The connection tubing and microfluidic device were sterilized by passing 1 mL 70% ethanol solution, followed by 1 mL of PBS buffer. The loaded syringes were then finger tightened onto male Luer connections and placed onto a Harvard 11 PLUS syringe pump. The flow rate is set to 8 μL/min for 5 min to purge air bubbles from the system, then the flow rate was lower to the experimental flow rate (0.2−0.6 μL/min) for 5 min to discard enough fluid before collecting cell clusters. Live cell images were obtained in situ at 10× magnification using an Olympus CKX41 microscope to record the size and growth of the clusters. The images of cell clusters were recorded at 0 mm, 7.5 mm, and 15.0 mm of the microfluidic channel to collect data of cluster size, while the flow rate and the cell density were changed to study the relationship between microtissue generation and microfluidic flow conditions as shown in the 3D plot.

Confocal Microscopy of RFP/GFP 3D Coculture Microtissues. To obtain confocal images of coculture microtissues, GFP and RFP cells were grown to approximately 95% confluency and treated with oxyamine and ketone bearing liposomes, respectively, using our standard protocol. Engineered cells (250 μL, 2 × 10^6/mL) were immediately loaded into separate sterilized 1 mL gastight Luer lock Hamilton gas chromatography syringes, which were finger tightened onto male Luer connections and placed onto a Harvard 11 PLUS syringe pump. The flow rate was set to 8 μL/min for 5 min to purge air bubbles from the system, and then reduced to 0.4 μL/min for 5 min. After that, collection of cells was started. Flow experiments were performed for 3 h, before the collecting slides were transferred to tissue culture plates and incubated at 37 °C and 5% CO_2. After culturing the cell clusters for 12 h, cell samples were fixed with 3.8% formaldehyde, washed with PBS, and mounted onto thin glass slides with Light Diagnostics Mounting Fluid (Millipore) for 3D confocal microscopy using a Zeiss LSM 700.

Confocal Microscopy of Three-Cell Lines (Red/Green/Blue) Microtissues. To generate three-cell line microtissues and observe by confocal microscopy, oxyamine engineered C3*H*/10T1/2 cells were treated with 0.3% v/v of CellTracker Blue CMAC (Life Technologies) for 45 min, and then mixed with ketone engineered GFP cells and RFP cells. Blue-stained C3*H*/10T1/2 cells presenting oxyamine (4 × 10^6/mL) were loaded into a 1 mL Hamilton glass syringe, while ketone engineered GFP cells (2 × 10^6/mL) and ketone engineered RFP cells (2 × 10^6/mL) were loaded into another 1 mL Hamilton glass syringe. The two syringes were connected to the microfluidic device and flow rate was controlled at 0.4 μL/min. Cell clusters were dispensed onto 1 cm^2 glass slides for 45 min and then incubated in tissue culture plates for 12 h at 37 °C with 5% CO_2. Cell samples were fixed with 3.8% formaldehyde, washed with PBS, and mounted onto thin glass slides with Light Diagnostics Mounting Fluid (Millipore) for 3D confocal microscopy using a Zeiss LSM 700.

3D Coculture Multilayers of HMSCs and 3T3 Fibroblasts. HMSCs and 3T3 fibroblasts were surface engineered with ketone and oxyamine liposomes, respectively. 3T3 fibroblasts presenting oxyamines were then trypsinized and added (1 × 10^5 cells/mL) to the hMSCs. These cells were cocultured in adipogenic, fibroblast, and osteoblast induction and maintenance media, resulting in the 3D multilayered, tissue-like structures of adipocytes, fibroblasts, osteoblasts, and 3T3 fibroblasts. After differentiation, the 3D coculture was fixed with formaldehyde (4% in PBS, 30 min). Substrates were then immersed in a solution containing water and 60% isopropyl alcohol (3−5 min), followed by staining with Oil Red O (5 min) and Harris Hemotoxylin (1 min). Substrates were visualized by phase contrast microscopy using a Zeiss inverted microscope. The substrates for fibroblast differentiation were fixed with formaldehyde and permeated with 0.1% Triton X-100. Monoclonal antibody of collagen I was applied for 1 h, and then incubated with secondary antibody anti-mouse IgG (FITC conjugate) for 30 min, followed by DAPI for 30 min for nucleus staining (reagents from Fisher Scientific). The substrates for osteogenic differentiation were stained with sigma Alkaline Phosphatase (ALP) kit (sigma kit 85).

Collagen Based RFP and GFP Tissue Formation. To make macro-size (2 × 2 cm^2) robust tissue, collagen was introduced. Oxyamine tailored GFP cells (2 mL, 4 × 10^6/mL) and ketone tailored RFP cells (2 mL, 4 × 10^6/mL) were loaded into the microfluidic device to generate RFP/GFP microtissue. The flow rate was set to 8 μL/min for 5 min to purge air bubbles from the system, and then reduced to 0.4 μL/min for 5 min. After that, collection of cells was started. The cell clusters were collected onto a 2 × 2 cm^2 slide loaded with liquid collagen solution. After collection, the collagen/cell hybrid was transferred to a tissue culture plate and incubated at 37 °C and 5% CO_2 for 30 min to allow the collagen solution to solidify. Cell culture media were then added and the collagen/cell hybrid tissue was incubated for 12 h before being peeled off the glass slide. The collagen supported macrotissue was then fixed with 3.8% formaldehyde, washed with PBS, and mounted onto thin glass slides with Light Diagnostics Mounting Fluid (Millipore) for 3D confocal microscopy using a Zeiss LSM 700.

3D Oriented Coculture Multilayers (RFP-GFP-RFP, thin). Microscope glass coverslips were cut into small pieces in advance and put into a 96-well microplate. RFP cells were grown on the slips in the microplate until 95% confluency was reached. Through standard liposome treatment, the RFP cells were surface engineered to present ketone group. GFP cells presenting oxyamine (200 μL, 5 × 10^5/mL) were then loaded by standard microfluidics procedure onto the ketone tailored RFP cells, and then cultured for 12 h. After removing most media, ketone tailored RFP cells (200 μL, 5 × 10^5/mL) were loaded onto 1 cm^2 glass slides by microfluidics, and cultured for 6 h. The slides were then gently picked up and fixed in 3.8% formaldehyde, washed with PBS, and mounted onto thin glass slides with Light Diagnostics Mounting Fluid (Millipore) for 3D confocal microscopy using a Zeiss LSM 700.

3D Oriented Coculture Multizones (RFP-GFP-RFP, thick). Microscope glass coverslips were cut into small pieces in advance and put into a 96-well microplate. Ketone tailored RFP cells (150 μL, 1 × 10^6/mL) and oxyamine tailored RFP cells (150 μL, 1 × 10^6/mL) were loaded by standard microfluidics procedure onto the coverslips in the microplate, and cultured for 12 h. After removing most media, ketone tailored GFP cells (150 μL, 1 × 10^6/mL) and oxyamine tailored GFP cells (150 μL, 1 × 10^6/mL) were loaded by microfluidics onto the RFP cells, and then cultured for 12 h. After removing most media, ketone tailored RFP cells (150 μL, 1 × 10^6/mL)

DOI: 10.1021/acs.bioconjchem.5b00376
Bioconjugate Chem. 2015, 26, 1939−1949

and oxyamine tailored RFP cells (150 μL, 1 × 10^6/mL) were loaded by microfluidics again, and cultured for 6 h. The slides inside the microplate were then gently picked up and fixed in 3.8% formaldehyde, washed with PBS, and mounted onto thin glass slides with Light Diagnostics Mounting Fluid (Millipore) for 3D confocal microscopy using a Zeiss LSM 700.

Oxime Bond Formation (Synthesis of 2-(Propan-2-ylideneaminooxy)acetic acid). To a 10 mL flask with magnetic stir bar, 1.1 mmol, 91.03g/mol, 100 mg) of *o*-(carboxymethyl)hydroxylamine hemihydrochloride was added and purged with argon gas. Freshly distilled acetone (3 mL) was then added by syringe and stirred at room temperature for 4 h. Excess acetone was removed by rotary evaporator to give (140 mg, 131.06 g/mol, 99%) conversion to the oxime product 2-(propan-2-ylideneaminooxy)acetic acid as a white solid. ^{1}H NMR (D_2O, 300 MHz): δ 4.45 (s, 2H), 1.85 (s, 3H), 1.79 (s, 3H); ^{13}C NMR (D_2O, 400 MHz): δ 175.45, 160.82, 69.81, 20.61, 15.31.

Oxime Hydrolysis Analysis. Oxime hydrolysis experiments were conducted by adding 1.5 mg (11 μmol) of 2-(propan-2-ylideneaminooxy)acetic acid into five separate scintillation vials, followed by preparation of 0.1 M buffered D_2O solutions using pyridine (pH 11.0), sodium bicarbonate (pH 8.0), PBS (pH 7.4), sodium carbonate (pH 5.0), and sodium formate (pH 3.0), respectively. Once the five separate samples of 2-(propan-2-ylideneaminooxy)acetic acid were dissolved in 0.5 mL of the different pH buffered D_2O solutions, their respective NMR spectra were taken (ns = 8). Data was gathered initially at 3 h intervals, followed by once a day, then once a week to determine the rate of hydrolysis of the starting material.

Oxime Formation Kinetics Conditions. Pseudo-first-order rate experiments were conducted using ^{1}H NMR (300 MHz) spectroscopy. These experiments were performed in typical NMR tubes by dissolving methoxyamine hydrochloride (1.5 mg, 83.52 g/mol, 18 μmol) and freshly distilled acetone (150 μL, distilled over dririte) in 0.25 mL PBS buffered D_2O (pH 7.4) at 37.0 °C, respectively. The two solutions were quickly mixed together in the NMR tube and placed into the spectrometer, and the first time point was immediately taken, with subsequent data points taken every 40 s. This experiment was repeated using 2-(propan-2-ylideneaminooxy)acetic acid (11 mg, 109.30 g/mol, 11 μmol) dissolved in 0.25 mL PBS buffered D_2O (pH 7.4) in a NMR tube at 37.0 °C, and freshly distilled acetone was added into 0.25 mL PBS buffered D_2O (pH 7.4) and warmed to 37.0 °C. The two solutions were then mixed in a NMR tube followed by placement into a spectrometer and the first time point was immediately taken, with subsequent data points taken every 40 s.

Stem Cell Differentiation in Coculture. RT-PCR Analysis. Human mesenchymal stem cells (hMSCs) were induced to differentiate for 2 weeks. Total RNA was then extracted by RNA isolation kits (Qiagen). 1 μg of total RNA was converted to cDNA using AMV reverse transcriptase and random hexamer primers (Promega). The resulting cDNA was used in PCR with the following primer, LPL (sense 5′-GAG ATT TCT CTG TAT GGC ACC-3′, antisense 5′-CTG CAA ATG AGA CAC TTT CTC-3′), PPARγ2 (sense 5′-GCT GTT ATG GGT GAA ACT CTG-3′, antisense 5′-ATA AGG TGG AGA TGC AGG CTC-3′), Collagen I (sense 5′-TGC TGG CCA ACC ATG CCT CT-3′, antisense 5′-TTG CAC AAT GCT CTG ATC-3′), Collagen II (sense 5′-ATG ACA ACC TGG CTC CCA AC-3′, antisense 5′-GCC CTA TGT CCA CAC CGA-3′), RUNX2 (sense 5′-GAT GAC ACT GCC ACC TCT GAC TT-3′, antisense 5′-CCC CCC GGC ACC ATG GGA AAC TG-3′), ALPL (sense 5′-CCA TTC CCA CGT CTT CAC ATT-3′, antisense 5′-GAG GGC CAG CGC GAG CAG CAG GG-3′), at annealing temperatures of 52 °C, 55 °C, 53 °C, 57 °C, 61 °C, 66 °C, respectively. Amplification reactions were carried out for 1 min through 30 cycles, and the reaction products were subjected to 1% agarose gel electrophoresis. The reaction products are 276bp (Lpl), 351bp (PPARγ2), 489bp (Collagen I), 359bp (Collagen II), 362bp (RUNX2), and 418bp (ALPL), respectively.

Bubble Fusion via Oxime Chemistry. Supporting Movies S1, S2: Commercially available soap bubble toys were obtained from Crayola. Control experiment was performed by directly using the commercial soap solutions for blowing and merging bubbles (Movie S1)—resulting in no fusion—only bubble adhesion. A second experiment was performed based on the same soap solutions but doped with 5% *O*-dodecyloxyamine and 5% 2-dodecanone, respectively (Movie S2)—resulting in bubble fusion via an interfacial oxime ligation.

Spheroid Assembly. Supporting Movies S3, S4: Microfluidic device was mounted on a Zeiss AXIO Observer Inverted Fluorescence Microscope. Ketone engineered GFP cells (2 × 10^6/mL) and oxyamine engineered GFP cells (2 × 10^6/mL) were prepared in PBS and loaded into the Hamilton glass syringes separately. The two syringes were connected to the microfluidic device and flow rate was controlled at 0.4 μL/min. Live recording of the two cell populations flowed through the microfluidic channels were taken automatically by the microscope (Movie S3). Control experiment was identical but without liposome fusion of bio-orthogonal groups to the cells (Movie S4). This resulted in only single cells floating through the channel and no spheroid assemblies observed.

■ ASSOCIATED CONTENT

Supporting Information

The Supporting Information is available free of charge on the ACS Publications website at DOI: 10.1021/acs.bioconjchem.5b00376.

Supporting figures S1−S4 describe tissue viability and spheroid viability studies (PDF)

Cell−cell interaction in microfluidic channels—bubble fusion in oxime chemistry (AVI)

Cell−cell interaction in microfluidic channels—bubble fusion in oxime chemistry (AVI)

Cell−cell interaction in microfluidic channels—spheroid assembly (AVI)

Cell−cell interaction in microfluidic channels—spheroid assembly (AVI)

■ AUTHOR INFORMATION

Corresponding Author

*E-mail: mnyousaf@yorku.ca; chrchem@yorku.ca.

Notes

The authors declare no competing financial interest.

■ ACKNOWLEDGMENTS

This work was supported by National Science and Engineering Research Council (NSERC) of Canada, Canadian Foundation for Innovation (CFI) and a NSERC CREATE grant (Canada). We also thank Professors Milan Mrkisch (Northwestern), Wenbin Lin (Univ. Chicago), Axel Guenther (Univ. Toronto),

DOI: 10.1021/acs.bioconjchem.5b00376
Bioconjugate Chem. 2015, 26, 1939−1949

Leaf Huang (UNC Chapel Hill) and Mike Ramsey (UNC Chapel Hill) for their insightful comments and suggestion.

REFERENCES

(1) Gartner, Z. J., and Bertozzi, C. R. (2009) Programmed assembly of 3-dimensional microtissues with defined cellular connectivity. *Proc. Natl. Acad. Sci. U. S. A. 106*, 4606−4610.
(2) Gong, P., Zheng, W., Huang, Z., Zhang, W., Xiao, D., and Jiang, X. (2013) A strategy for the construction of controlled three-dimensional multilayered tissue like structures. *Adv. Funct. Mater. 23*, 42−46.
(3) Matsunaga, Y. T., Morimoto, Y., and Takeuchi, S. (2011) Molding cell beads for rapid construction of macroscopic 3D tissue architecture. *Adv. Mater. 23*, H90−H94.
(4) Sutherland, R. M. (1988) Cell and environment interactions in tumor microregions: the multicell spheroid model. *Science 240*, 177−184.
(5) Gottfried, E., Kunz-Schughart, L. A., Andreesen, R., and Kreutz, M. (2006) Brave little world - Spheroids as an in vitro model to study tumor-immune-cell interactions. *Cell Cycle 5*, 691−695.
(6) Macdonald, H. R., Howell, R. L., and Mcfarlane, D. L. (1978) The multicellular spheroid as a model tumol allograft. *Transplantation 25*, 141−145.
(7) Torisawa, Y. S., Takagi, A., Nashimoto, Y., Yasukawa, T., Shiku, H., and Matsue, T. (2007) A multicellular spheroid array to and viability realize spheroid formation, culture, assay on a chip. *Biomaterials 28*, 559−566.
(8) Tejavibulya, N., Youssef, J., Bao, B., Ferruccio, T. M., and Morgan, J. R. (2011) Directed self-assembly of large scaffold-free multi-cellular honeycomb structures. *Biofabrication 3*, 034110.
(9) Selden, N. S., Todhunter, M. E., Jee, N. Y., Liu, J. S., Broaders, K. E., and Gartner, Z. J. (2012) Chemically programmed cell adhesion with membrane anchored oligonucleotides. *J. Am. Chem. Soc. 134*, 765−768.
(10) Lutolf, M. P., and Hubbell, J. A. (2005) Synthetic biomaterials as instructive extracellular microenvironments for morphogenesis in tissue engineering. *Nat. Biotechnol. 23*, 47−55.
(11) Peng, Y., Kim, D. H., Jones, T. M., Ruiz, D. I., and Lerner, R. A. (2013) Engineering cell surfaces for orthogonal selectability. *Angew. Chem., Int. Ed. 52*, 336−340.
(12) Huang, L., Lu, G., Hao, J., Wang, H., Yin, D., and Xie, H. (2013) Enveloped virus labeling via both intrinsic biosynthesis and metabolic incorporation of phospholipids in host cells. *Anal. Chem. 85*, 5263−5270.
(13) Ott, C. H., Matthiesen, S. T., Goh, S. K., Black, L. D., Kren, M. S., Netoff, I. T., and Taylor, A. D. (2008) Perfusion-decellularized matrix: using nature's platform to engineer a bioartificial heart. *Nat. Med. 14*, 213−221.
(14) Torchilin, V. P. (2005) Recent advances with liposomes as pharmaceutical carriers. *Nat. Rev. Drug Discovery 4*, 145−160.
(15) Csiszar, A., Hersch, N., Dieluweit, S., Biehl, R., Merkel, R., and Hoffmann, B. (2010) Novel fusogenic liposomes for fluorescent cell labeling and membrane modification. *Bioconjugate Chem. 21*, 537−543.
(16) Chen, Y. F., Sun, T. L., Sun, Y., and Huang, H. W. (2014) Interaction of daptomycin with lipid bilayers: a lipid extracting effect. *Biochemistry 53*, 5384−5392.
(17) Chan, Y. H. M., and Boxer, S. G. (2007) Model membrane systems and their applications. *Curr. Opin. Chem. Biol. 11*, 581−587.
(18) Bertozzi, C. R. (2011) A decade of bioorthogonal chemistry. *Acc. Chem. Res. 44*, 651−653.
(19) McKay, C. S., and Finn, M. G. (2014) Click chemistry in complex mixtures: bioorthogonal bioconjugation. *Chem. Biol. 21*, 1075−1101.
(20) Dieterich, D. C., Lee, J. J., Link, A. J., Graumann, J., Tirrell, D. A., and Schuman, E. M. (2007) Labeling, detection and identification of newly synthesized proteomes with bioorthogonal non-canonical amino-acid tagging. *Nat. Protoc. 2*, 532−540.
(21) Shui, L. L., Bomer, J. G., Jin, M. L., Carlen, E. T., and van den Berg, A. (2011) Microfluidic DNA fragmentation for on-chip genomic analysis. *Nanotechnology 22*, 494013.
(22) Autebert, J., Coudert, B., Bidard, F. C., Pierga, J. Y., Descroix, S., Malaquin, L., and Viovy, J. L. (2012) Microfluidic: an innovative tool for efficient cell sorting. *Methods 57*, 297−307.
(23) Günther, A., and Jensen, K. F. (2006) Multiphase microfluidics: from flow characteristics to chemical and materials synthesis. *Lab Chip 6*, 1487−1503.
(24) Watts, P., and Haswell, S. J. (2003) Microfluidic combinatorial chemistry. *Curr. Opin. Chem. Biol. 7*, 380−387.
(25) Dutta, D., Pulsipher, A., Luo, W., Mak, H., and Yousaf, M. N. (2011) Engineering cell surfaces via liposome fusion. *Bioconjugate Chem. 22*, 2423−2433.
(26) Dutta, D., Pulsipher, A., Luo, W., and Yousaf, M. N. (2011) Synthetic chemoselective rewiring of cell surfaces: generation of three-dimensional tissue structures. *J. Am. Chem. Soc. 133*, 8704−8713.
(27) Pulsipher, A., Dutta, D., Luo, W., and Yousaf, M. N. (2014) Cell-surface engineering by a conjugation-and-release approach based on the formation and cleavage of oxime linkages upon mild electrochemical oxidation and reduction. *Angew. Chem., Int. Ed. 53*, 9487−9492.
(28) Luo, W., Pulsipher, A., Dutta, D., Lamb, B. M., and Yousaf, M. N. (2014) Remote control of tissue interactions via engineered photoswitchable cell surfaces. *Sci. Rep. 4*, 6313.
(29) Nicolson, G. L. (2014) The Fluid—Mosaic Model of Membrane Structure: Still relevant to understanding the structure, function and dynamics of biological membranes after more than 40 years. *Biochim. Biophys. Acta, Biomembr. 1838*, 1451−1456.
(30) Kelkar, S. S., and Reineke, T. M. (2011) Theranostics: combining imaging and therapy. *Bioconjugate Chem. 22*, 1879−1903.
(31) Patterson, D. M., Nazarova, L. A., and Prescher, J. A. (2014) Finding the right (bioorthogonal) chemistry. *ACS Chem. Biol. 9*, 592−605.
(32) Drake, C. G., Lipson, E. J., and Brahmer, J. R. (2013) Breathing new life into immunotherapy: review of melanoma, lung and kidney cancer. *Nat. Rev. Clin. Oncol. 11*, 24−37.
(33) Groeber, F., Holeiter, M., Hampel, M., Hinderer, S., and Schenke-Layland, K. (2011) Skin tissue engineering − in vivo and in vitro applications. *Adv. Drug Delivery Rev. 63*, 352−366.
(34) Bhatia, S. N., Underhill, G. H., Zaret, K. S., and Fox, I. J. (2014) Cell and tissue engineering for liver disease. *Sci. Transl. Med. 6*, 245−254.
(35) Vunjak-Novakovic, G., Tandon, N., Godier, A., Maidhof, R., Marsano, A., Martens, T. P., and Radisic, M. (2010) Challenges in cardiac tissue engineering. *Tissue Eng., Part B 16*, 169−187.
(36) Murphy, S. V., and Atala, A. (2014) 3D bioprinting of tissues and organs. *Nat. Biotechnol. 32*, 773−785.
(37) Luo, W., Westcott, N., Dutta, D., Pulsipher, A., Rogozhnikov, D., Chen, J., and Yousaf, M. N. (2015) *ACS Chem. Biol.* [Online early access] DOI: 10.1021/acschembio.5b00137.

DOI: 10.1021/acs.bioconjchem.5b00376
Bioconjugate Chem. 2015, 26, 1939−1949